REPORT

UV Resonance Raman Spectroscopy

for Analytical, Physical, and Biophysical Chemistry

Part 1

Sanford A. Asher
Department of Chemistry
University of Pittsburgh
Pittsburgh, PA 15260

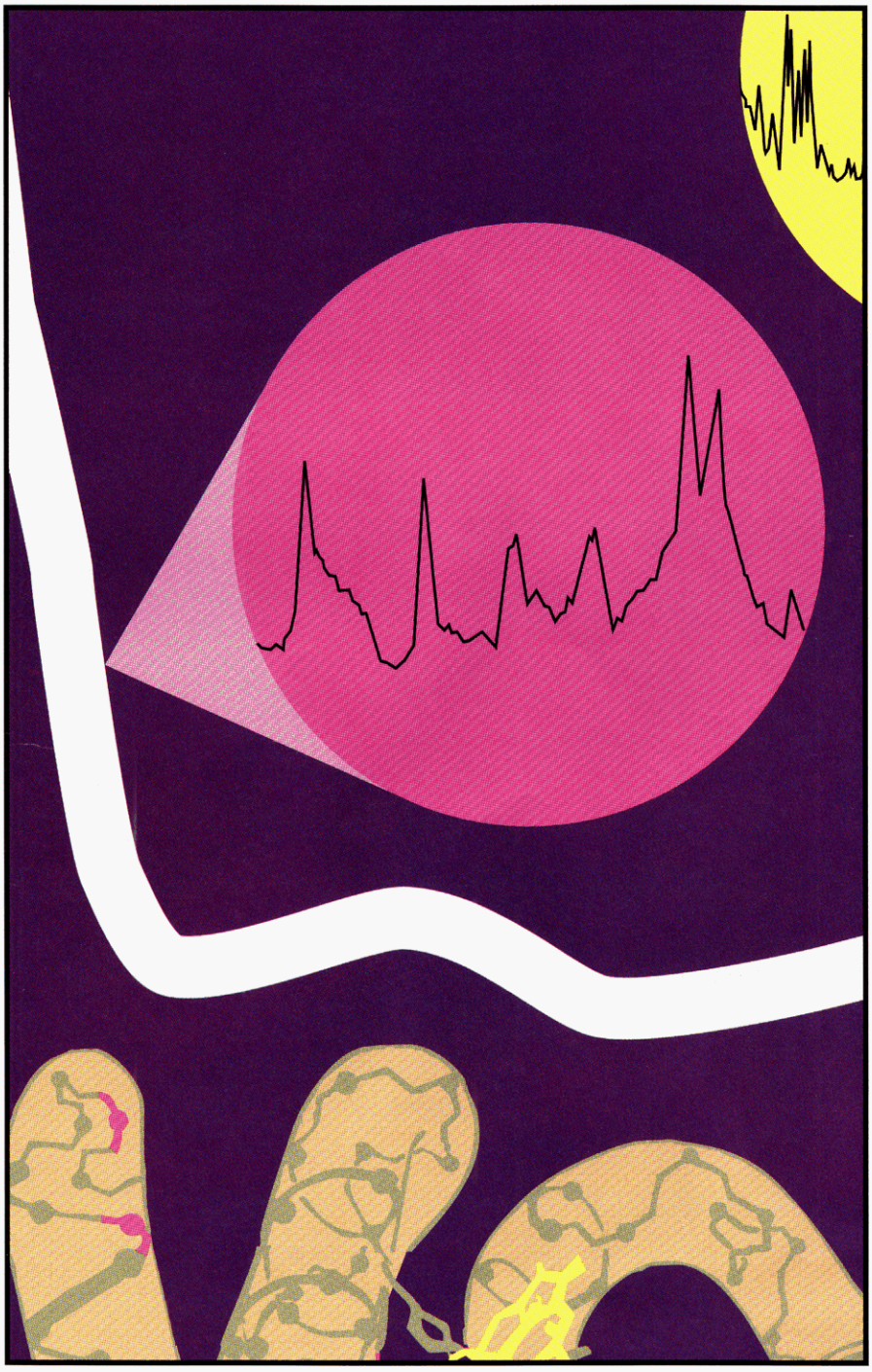

Raman spectroscopy measures the magnitudes and intensities of frequency shifts that occur because of the inelastic scattering of light from matter (*1*, *2*). The observed shifts can be used to extract information on molecular structure and dynamics. In addition, important information can be obtained by measuring the change in the electric field orientation of the scattered light relative to that of the incident exciting light.

The experiment is usually performed by illuminating a sample with a high-intensity light beam with a well-defined frequency and a single linear polarization (Figure 1); the scattered light is collected over some solid angle and measured to determine frequency, intensity, and polarization. The inelastic scattering Raman phenomenon, which leads to frequency shifts, is phenomenologically distinct from the relaxed emission denoted as fluorescence (Figure 2) because the inelastic scattering is a single event, and a real emitting excited state is never created.

In contrast, relaxed fluorescence emission (Figure 2) occurs through the population of an excited state, which can subsequently undergo vibrational relaxation prior to fluorescence back to the ground state. The distinction between fluorescence and Raman scattering is more subtle for excitation within the absorption bands of small molecules in the gas phase, where single vibrational-level fluorescence can occur from well-defined vibronic levels (*3*).

The Raman effect is named after Sir C. V. Raman. In his classic 1928 paper, coauthored by K. S. Krishnan, Raman described experimental observations of the inelastic scattering

0003-2700/93/0365-59A/$04.00/0

of sunlight from vibrational quantum levels of numerous liquids (*1*). Raman received the Nobel prize for his work. The possibility of inelastic scattering of light from discrete quantum levels of matter was envisioned in 1923 by A. Smekal (*1*).

Much of the early work centered on vibrational Raman scattering; these studies were central to developing a fundamental understanding of molecular structure and vibrational motion. Before 1945 it was much easier to take Raman spectroscopic measurements than to take mid-IR absorption measurements. Raman excitation used Hg arc emission lines and photographic detection. After 1945 the advent of relatively convenient IR instrumentation decreased enthusiasm for Raman spectroscopy, and it became a specialized field. Much of the work before 1960 centered on examining molecular structure and molecular vibration dynamics. Major advances occurred during this period in the theoretical understanding of Raman spectroscopy and in the resonance Raman phenomenon, where excitation occurs within an electronic absorption band. The first commercial Raman instrument became available in 1953.

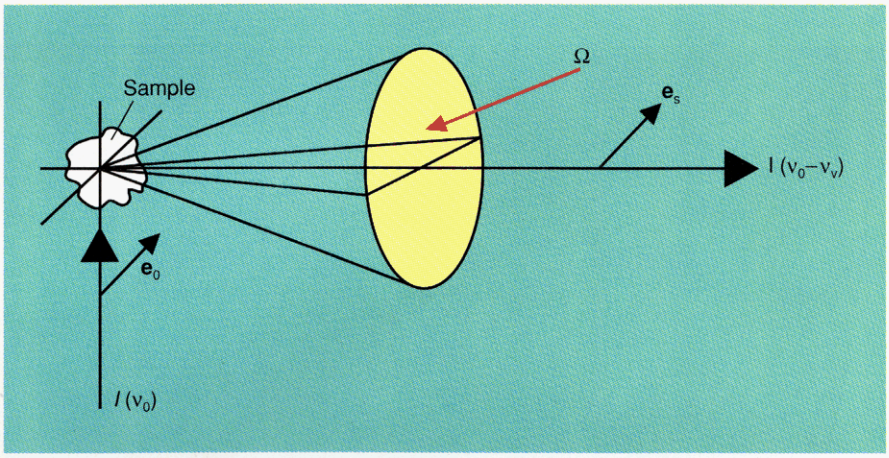

Figure 1. Raman inelastic light-scattering process showing excitation of a sample with light of an intensity $I(\nu_0)$ and frequency ν_0.

The incident light has an electric field of magnitude and direction shown by $\mathbf{e}_0$. Raman scattered light at a frequency $\nu_0 - \nu_v$ (ν_v is the Raman active molecular vibrational frequency) and intensity $I(\nu_0 - \nu_v)$ is collected over the solid angle Ω. A ray of this light is shown with its electric field polarized along $\mathbf{e}_s$ parallel to the incident field.

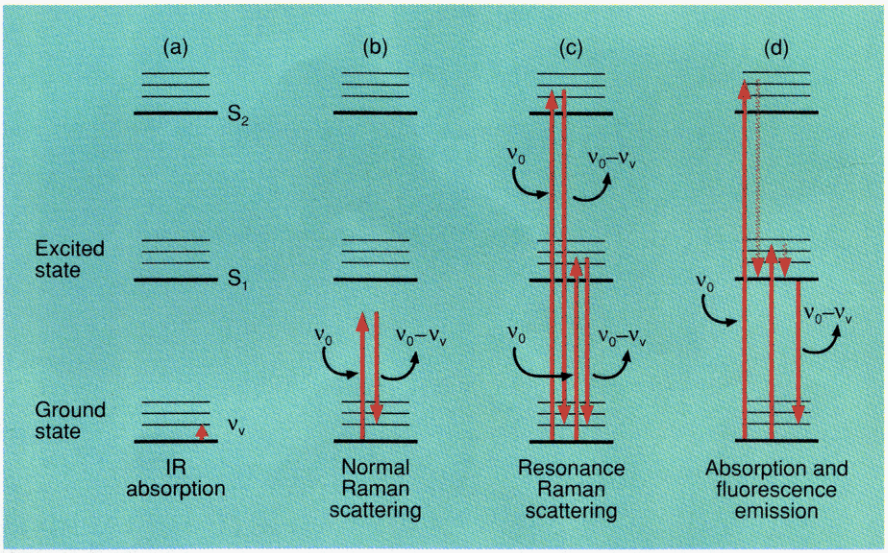

Figure 2. IR absorption and Raman scattering.

(a) Vibrational IR absorption. (b) Inelastic scattering of light of frequency ν_0 to a frequency of $\nu_0 - \nu_v$. The shift in frequency corresponds to a vibrational frequency in this case, and the scattering is known as vibrational Raman scattering. Because the excitation occurs at a frequency far removed from any absorption bands associated with excitations to electronic excited states, the phenomenon is known as normal, or nonresonance, Raman scattering. (c) Excitation occurring within an electronic transition produces resonance Raman scattering. (d) Absorption and fluorescence emission in which an excited state is created. Typical relaxed fluorescence occurs subsequent to the population of an excited state. Prior to emission, this excited state quickly relaxes to the lowest vibrational level of the lowest singlet excited electronic state. Emission is broad and the molecule undergoes a transition to different vibronic levels of the ground state.

The advent of the photomultiplier tube and the He–Ne laser caused a resurgence of interest. In 1928, 58 papers were published on Raman spectroscopy; by 1937, the total was 1785. Between 1987 and 1989, for example, more than 6000 papers were published with the word Raman in their title (*4*). Raman spectroscopy has become a major tool for fundamental studies in physics and physical chemistry as well as for applied studies in the biological sciences and analytical chemistry.

During the 1970s most Raman instrumentation used Ar^+ lasers with excitation between 450 and 520 nm—a region that, unfortunately, is especially prone to interference from fluorescent impurities. The interferences degrade signal-to-noise ratios (S/N), resulting in poor spectra for many complex samples. Many Raman studies involved pure compounds or those samples that proved amenable to visible excitation.

The usefulness of Raman spectroscopy for studying aqueous samples, especially biological samples, was appreciated early on. Because the Raman scattering of water is very weak, it is easy to study species in aqueous environments. IR measurements, in contrast, often suffer from water interferences that cannot be overcome. In 1972 an important paper by T. C. Strekas and T. G. Spiro (*5*) demonstrated the usefulness of the resonance Raman effect in selective studies of the chromophoric hemes of hemoglobin and myoglobin. Very high spectral S/N were obtained from heme protein samples at relatively low concentrations. This technique was quickly adopted by those researchers interested in biological problems. Amazing progress has been made over the past 20 years using this technique to, for example, study heme protein structure and function (*6*) and to elucidate the photochemical mechanisms of visual pigments such as rhodopsin (*7*). Until recently, however, resonance Raman spectroscopy was limited to the small subset of compounds absorbing in the visible or near-UV spectral regions where laser sources typically have been available.

Continuing advances in methods fueled numerous studies in which molecular structure in the gas, liq-

uid, and solid phases was examined. The advent of surface-enhanced Raman spectroscopy (*8*) opened the door to studying extremely low concentrations of molecules on surfaces. Nonlinear Raman techniques, such as coherent anti-Stokes Raman spectroscopy, were used to study combustion processes (*1*).

The 1980s saw even more rapid advancements, such as the development of UV-Raman spectroscopy and of FT-Raman spectroscopy (*9*), which uses near-IR excitation. These extensions into spectral regions away from the visible have dramatically increased the utility and applicability of Raman spectroscopy.

In FT-Raman spectroscopy, the multiplex advantage of the Michelson interferometer is used to increase the spectral S/N that is limited by IR detector background noise. FT-Raman spectroscopy has the advantage of excitation in a spectral region that is much less susceptible than visible excitation to fluorescent interferences. Relative intensities from vibrations of different species are roughly proportional to concentrations of those species in the sample, and the Raman-active vibrations have roughly similar intensities. For example, aromatic ring vibrations have intensities similar to those of aliphatic C–C stretching vibrations, which have intensities similar to those of C–H stretching vibrations.

In contrast, UV-Raman spectroscopy uses selective excitation in the UV absorption bands of molecules to produce spectra of particular analytes and chromophoric segments of macromolecules. Resonance excitation has the advantage of selectivity. In addition, UV-Raman measurements of condensed-phase samples excited below 260 nm are not plagued by fluorescent interferences (*10*).

In this article, the first in a two-part series, phenomenology, instrumentation, and fundamental applications will be discussed. In Part II, which will appear in the Feb. 15 issue of ANALYTICAL CHEMISTRY, analytical applications, biological studies, new methods, and future developments will be discussed.

Phenomenology

Figure 3 illustrates the Raman scattering phenomenon. An incident electromagnetic field drives the electron cloud of the molecule at the incident frequency ν_0. An oscillating dipole moment is created by the resulting displacement of electronic charge. Because the charge is accelerating, it radiates energy in the form of electromagnetic radiation. The radiated frequency ν_0 is identical to the excitation frequency; light is elastically scattered. If the scattering species is small compared with the wavelength of light, the scattering is known as Rayleigh scattering. Because charge acceleration induces the radiation, the Rayleigh scattering efficiency increases with the fourth power of the excitation frequency. This phenomenon explains why the sky is blue and the setting (or rising) sun is red.

Other dynamic processes modulate the induced oscillating dipole moment. As shown in Figure 3, a nuclear vibrational motion causes an oscillation of the electron cloud at frequency ν_v. The electron cloud oscillation at ν_0 couples to the vibrationally induced electron cloud oscillation at ν_v to give rise to a beat oscillation at $\nu_0 \pm \nu_v$, which radiates Raman scattered light at this frequency. Those vibrations that most efficiently Raman scatter are those that couple most effectively to the oscillating electron dipole moment induced by the exciting electromagnetic field.

There are particular excitation frequencies that are natural frequencies of oscillation of specific electron oscillators of the molecular electron cloud. These natural frequencies are the molecular electronic absorption band frequencies. Excitation at these frequencies is said to be in "resonance" with the electronic transition (Figure 2); therefore, the Raman scattering is said to be "resonance Raman" scattering. This resonance excitation at the natural frequency of electron cloud oscillation results in an increased oscillating charge displacement and a corresponding increase in the induced dipole moment; this, in turn, directly results in an increased scattering or reradiation efficiency for Raman scattering. The enhancement factor of resonance Raman scattering compared with that of normal Raman scattering can be as high as 10^8.

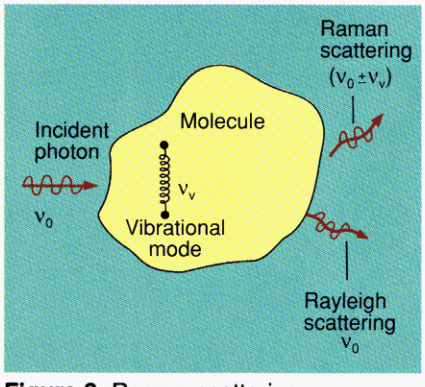

Figure 3. Raman scattering phenomenon.

The presence of a vibration at frequency ν_v is shown by the spring. Light scattered at $\nu_0 - \nu_v$ is known as Stokes Raman scattering; light scattered at $\nu_0 + \nu_v$ is known as anti-Stokes Raman scattering.

The observed Raman band intensities at a particular excitation frequency depend on the degree to which a vibration modulates the molecular polarizability. In a classical sense, the magnitude of the induced dipole moment μ depends linearly on the molecular polarizability α and the incident electromagnetic field $\mathbf{E}$, giving $\mu = \alpha\mathbf{E}$. In the case of Raman scattering, the effective polarizability is not the static polarizability α; it is the Raman polarizability α^R associated with perturbation of the static polarizability by the Raman active vibration $\alpha_R = (\partial\alpha/\partial Q)_0 Q$, where Q is the normal vibrational mode displacement. For excitation at frequency ν_0, the Raman intensity I_{mn} observed over a unit solid angle for a transition between vibronic levels m and n in the electronic ground-state manifold is (*11*)

$$I_{mn} = \sigma^R N I_0 W(\Omega)$$

where σ^R (cm^2/molc steradian [sr]) is the total differential Raman cross section for a single gas-phase molecule integrated over the Raman peak bandwidth, I_0 is the incident excitation intensity (photons/cm^2 s) into a particular sample volume element of area dA and length dl, N is the number of molecules within that volume element, and $W(\Omega)$ is a parameter that details the optical geometry and includes factors such as the collected solid angle Ω and the spectrometer efficiency.

The resonance Raman effect can lead to important selectivity in Raman spectral measurements. Figure 4 shows the absorption spectrum of a sample with two absorption bands. Raman spectra are shown that are excited at a wavelength longer than any absorption band (Figure 4c, normal Raman) or within the two absorption bands (Figures 4a and 4b, resonance Raman). Excitation away from resonance (Figure 4c) results in comparable Raman intensities from all analytes. The typical scattering cross section is $\sigma^R = 10^{-30}$ cm^2/molc sr (or 1 μBarn/molc sr). (One Barn equals 10^{-24} cm^2.) Resonance excitation within an absorption band can lead to an immense Raman intensity increase. For example, we have measured a Raman cross section of ~50 Barns/molc sr for pyrene.

Figures 4a and 4b show an increased Raman intensity for resonance excitation. Different Raman spectra are observed with excitation in resonance versus not in resonance. In addition, different spectra are observed with resonance excitation within different sample absorption bands—for example, the resonance Raman spectrum in Figure 4a differs from that in Figure 4b. If these absorption bands derive from different analytes in the sample, we selectively enhance the vibrational Raman spectrum of different analytes as we change the excitation wavelength. The selectivity factor can be as large as 10^8.

If the different absorption bands derive from different segments of a molecule, by changing excitation wavelengths we change the segment of the molecule studied. In contrast, if the two absorption bands derive from the same chromophoric segment of a single molecule, the spectra will differ because of differences in the structure of the excited states associated with the two electronic transitions; the different excited states couple differently with the ground-state vibrational motion.

We can easily estimate the number of nonresonance Raman photons that can be detected from a 0.1 M solution of an analyte with a Raman cross section of 1 μBarn/molc sr, illuminated by an incident laser beam of 1 W of 514.5 nm light (2.6×10^{18} photons/s). For a typical case, the limiting aperture is the height of the intensified Reticon detector (2.5 mm), and the spectrometer *f*/#. Let us assume the spectrometer is *f*/7.0, with a slit width of 200 μm, and the collection optic has a magnification of 6. For this case, the laser beam can be efficiently imaged into a column with a 33-μm (maximum) diameter and a 417-μm height that contains 2.2×10^{13} molecules. Ideally, we can collect 0.86 sr of the scattered light. According to the equation, if the spectrometer were 100% efficient, a total of 5.6×10^6 Raman photons/s would be detected for this vibration.

In contrast, the fluorescence cross section of an analyte with a molar absorptivity of 10^4 and a fluorescence quantum yield of 0.1 is equal to 3×10^{-22} cm^2/molc sr; 1.68×10^{15} fluorescence photons would be observed using the same instrument (assuming no self-absorption of the emitted light occurs).

Obviously, the fluorescence experiment is much more sensitive than the Raman experiment and we can observe the same amount of fluorescence signal as the Raman signal using a concentration 3×10^8-fold lower. However, in the case of resonance Raman scattering, Raman cross sections as high as ~ 10^{-22} cm^2/molc sr can occur. The resonance Raman sensitivity is comparable to that of fluorescence. Furthermore, sensitivity can be greater because the Raman spectrum has higher resolution.

Generally, numerous Raman bands exist, and all can be used to determine concentrations. The narrow Raman spectral bands carry a great deal of information on molecular structure, in contrast to the broad fluorescence emission. Also, the Raman cross sections are much less de-

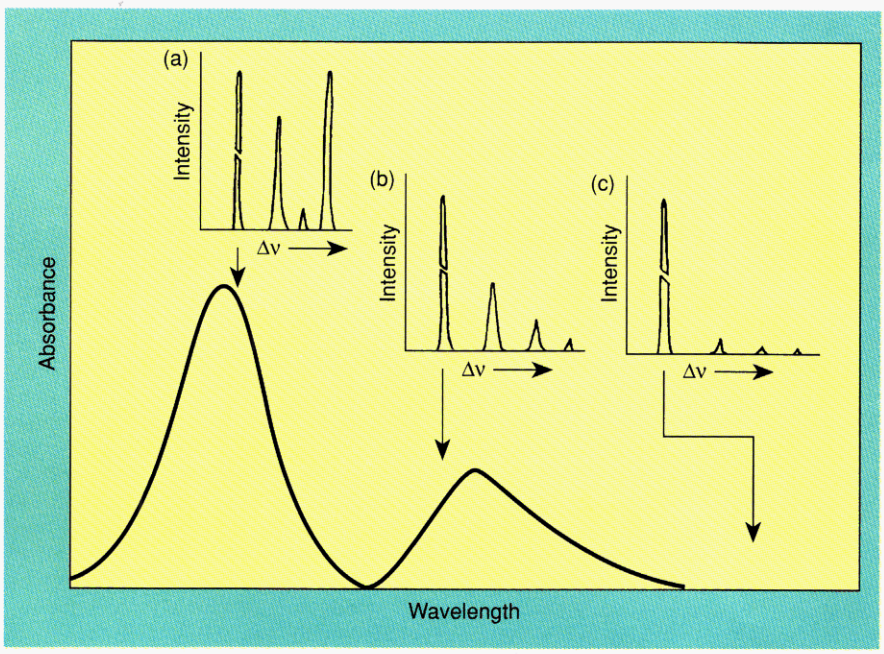

Figure 4. Selectivity available from resonance Raman spectroscopy.

The absorption spectrum is shown for a sample with two absorption bands. These bands could derive from two different analytes, two different chromophoric segments of a macromolecule, or two different electronic transitions of a single molecule. Three different Raman spectra are shown that derive from resonance Raman excitation within either of the two absorption bands (a and b) or from excitation away from the absorption (c). Excitation within resonance leads to much more intense Raman spectra. The most intense feature is the Rayleigh scattering band.

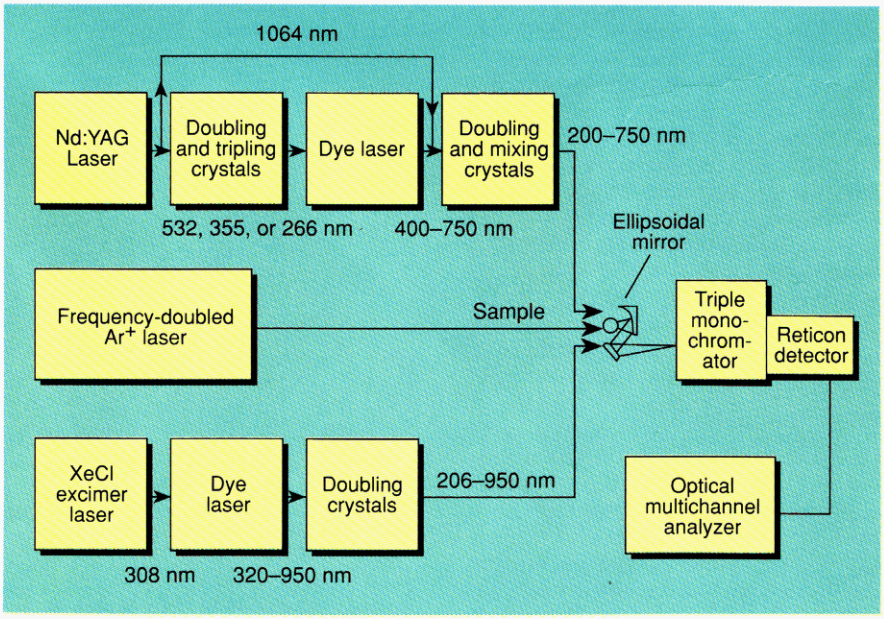

Figure 5. Diagram of basic instrumentation used for UV resonance Raman spectroscopy.

pendent on environment than are the fluorescence quantum yields. Modest changes in solvent composition can cause dramatic changes in fluorescence quantum yields, because the quantum yields are very sensitive to relatively small changes in fluorescence lifetimes. Thus, resonance Raman measurements can be very sensitive, the spectra can provide a great deal of molecular structural and environmental information, and an increased selectivity results from the ability to excite particular species.

Instrumentation

UV-Raman instrumentation has evolved rapidly (Figure 5). The original laser source used a low repetition rate (20 Hz) Nd:YAG laser with ~5-ns frequency pulses that were doubled or tripled to pump a dye laser whose frequency was doubled or mixed with the Nd:YAG 1.06-μm fundamental wavelength to generate light between 200 and 400 nm (*12*). The minimum average output power available in this region is 20 mW; in some spectral regions, hundreds of milliwatts are available. Raman shifting of the Nd:YAG harmonics in H_2 gas can also generate numerous wavelengths in the UV, and this approach can be used to construct a simpler, inexpensive UV laser source.

The low duty cycle (10^{-7}) of the Nd:YAG laser represents a major limitation because the laser pulses cannot be focused into a sample volume that can be efficiently imaged into the Raman spectrometer. The Nd:YAG output occurs as ~5 ns pulses, at a repetition rate of ~20 Hz. An average power of 20 mW corresponds to a peak power level of ~200 kW, which can induce nonlinear optical phenomena in matter. A power flux value of 2.5 GW/cm^2 would occur if this beam were focused into a 100-μm-diameter spot size.

A partial solution to this low duty cycle is to use a higher repetition rate excimer laser to pump a dye laser whose output was frequency-doubled into the UV region (*13*). Modern high-power excimer lasers can have repetition rates between 200 and 500 Hz; at the highest repetition rates the 16-ns laser pulses result in a duty cycle of 8×10^{-6}. This partially alleviates the nonlinear optical phenomena and the sample ground-state depletion that both complicates the Raman spectral measurements and necessitates defocusing the laser excitation beam at the sample.

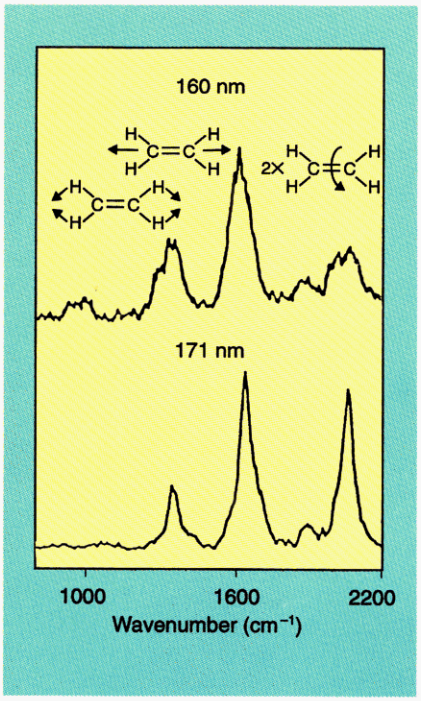

Figure 6. UV resonance Raman spectra of ethylene in the gas phase showing enhancement of the 1344-cm^{-1} C–H bending and the 1625-cm^{-1} C=C stretching vibrations and enhancement of the 2046-cm^{-1} overtone of the torsional vibration.

Different spectra are excited in the first excited singlet state of ethylene at 160 and 171 nm. The unique enhancement of this torsional overtone, whose fundamental is symmetry forbidden, indicates that the excited state is twisted. (Adapted with permission from Reference 20.)

An alternative approach uses a mode-locked Nd:YAG laser to create a quasi-continuous wave UV source with a duty cycle of 0.01 (*14*). A new laser has just become available that is ideal for Raman measurements that do not require continuous tuning (*15*). The Coherent Laser Group (division of Coherent, Inc.) has developed an intracavity frequency-doubled Ar^+ laser with five excitation wavelengths in the UV region: 257, 248, 244, 238, and 228.9 nm (400, 180, 400, 100, and 30 mW, respectively). This laser permits a major improvement in spectral S/N and, for the first time, allows UV-Raman studies of solid absorbing samples.

UV-Raman sample handling requires flowing the sample through the laser beam as a liquid jet, through a capillary, or along a waveguided stream. With pulsed lasers, it is essential to exchange each illuminated sample volume before the arrival of the next laser pulse to avoid sample heating; also, the high-energy UV photons might cause photochemical degradation in the samples. Most samples studied to date have not shown significant monophotonic photodegradation during the typical 10-min Raman measurement time.

The collection optics use either an ellipsoidal collection mirror for achromatic imaging or quartz lenses (when accurate relative intensity measurements are not essential). The typical spectrometer is a triple grating instrument in which the initial double monochromator operates in a subtractive configuration to filter out the Rayleigh scattered light. The third-stage spectrograph disperses and images the light onto a multichannel detector such as an intensified Reticon array. This multichannel detector is essential for simultaneous collection of the entire spectrum. A scanning system would have a far inferior S/N because most of the noise comes from the low-stability UV laser source. Charge-coupled detectors may eventually prove superior to the intensified Reticon detectors.

The triple spectrometer is inefficient; at best, only 7% of the Raman scattered light entering the entrance slit is transferred to the detector. Efforts are under way to use the more efficient single spectrograph (*16*); success requires very high quality, low stray light gratings, careful filtering of samples to minimize Rayleigh scattering, and careful optical imaging to avoid any reflections of the incident excitation beam into the spectrograph.

Fundamental applications

Investigations of the structure and dynamics of excited states of small molecules are an especially fertile area for UV-Raman investigations. Examination of the vibrations most enhanced by excitation in resonance with an electronic transition gives information on the excited-state structure and dynamics. The simplest rule of thumb is that resonance Raman-enhanced vibrations are those that distort the ground-state geometry toward the excited-state geometry. If the atomic motions involved in the enhanced vibrations are known, theoretical models can be applied to the measured Raman intensities to calculate the excited-state distortion. Numerous workers are using this information to examine the excited states of small molecules such as oxygen (*17a*), ammonia (*17b*), methyl iodide (*17c, 17e*), carbon disulfide (*17d*), ethylene (*18, 19*), and other species.

For methyl iodide (*17c*, *17e*), the excited state is dissociative and the Raman data give information on the short time dynamics of the photodissociation. For ethylene, excitation in the lowest allowed $\pi \rightarrow \pi^*$ transition (Figure 6) results in the unique enhancement of the overtone of a torsional vibration, in addition to the C=C double-bond stretch and the CH_2 bending vibration; the enhancement of this torsional vibration confirms that the ethylene excited state is twisted (*20*, *21*). Similar experiments examine the vibrational enhancement of stilbenes (*18*), for example, to determine the photochemical mechanism of photoisomerization. Interested readers are urged to examine the rapidly expanding literature on these insightful studies.

Another example that illustrates the power of the technique to probe excited states is a recent study we made to determine whether vinyls attached to hemes were conjugated into the aromatic porphyrin ring (Figure 7a) (*19*, *22*). This is an important question in biochemistry, because the hemes of hemoglobin have vinyl peripheral substituents and the protein may modulate the heme reactivity by controlling the vinyl group conjugation—possibly by altering the vinyl group geometry. In addition, vinyl group conjugation is relevant to electron transfer studies for porphyrins because the vinyl groups could represent a conduit for electron flow.

We were able to demonstrate the lack of vinyl group conjugation by measuring the extent of vinyl group C=C stretching enhancement with excitation in the UV region. Figure 7b shows the Raman spectrum of the (bis)cyanide complex of the heme. The strong peak at 1622 cm^{-1} in the heme complex comes from the C=C vinyl stretch; ^{13}C and deuterium vinyl substitution further confirm this assignment. Excitation of the heme in the UV region results in selective enhancement of the vinyl modes, and little enhancement occurs for the heme vibrational modes. The vinyl Raman cross sections are similar to that of the C=C group in 1-hexene (*19*), which indicates that the vinyl groups are not conjugated with the heme ring π electrons. If the vinyl were conjugated, its $\pi \rightarrow \pi^*$ transition would be intimately mixed with the heme transitions; no selective vinyl enhancement would occur with UV excitation.

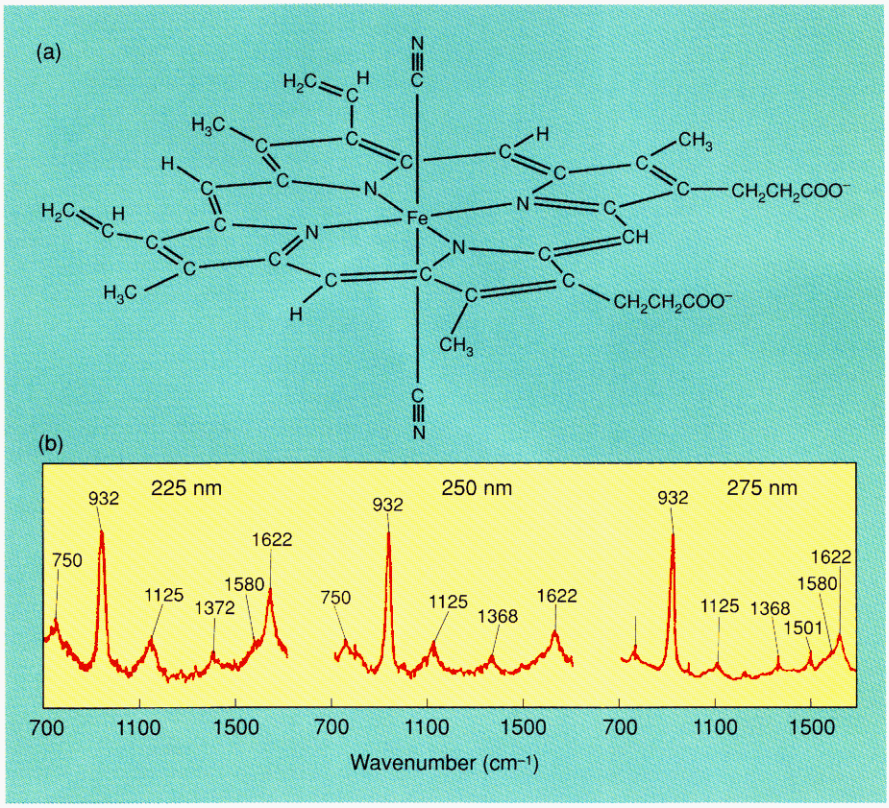

Figure 7. (a) Structure and (b) UV resonance Raman spectra of the bis(cyanide) ferric protoporphyrin IX complex.

The 932-cm^{-1} band is from the internal standard ClO_4. The selective UV enhancement of the vinyl C=C stretch at 1622 cm^{-1} and the band at 1125 cm^{-1} is evident from their relative intensity increases compared with that of the ClO_4 band as the excitation moves farther into the UV region. The band at 1125 cm^{-1} derives from a vibration with a major contribution of motion of the vinyl against the heme ring. Little enhancement occurs for the heme ring vibrations such as the 1368 cm^{-1} ν_4 ring breathing motion. This selective enhancement of the vinyl vibrations in the UV indicates the existence of a vinylic $\pi \rightarrow \pi^*$ transition at $\lambda < 220$ nm; the existence of this vinyl $\pi \rightarrow \pi^*$ transition indicates the absence of vinyl–heme conjugation. (Adapted from Reference 19.)

References

(1) Long, D. A. *Raman Spectroscopy*; McGraw-Hill Int. Book Co.: New York, 1977.
(2) a. Asher, S. A. *Ann. Rev. Phys. Chem.* **1988**, *39*, 537–88. b. Harada, I.; Takeuchi, H. In *Spectroscopy of Biological Systems*; Clark, R. T.; Hester, R. E., Eds.; John Wiley and Sons: New York, 1986. c. Hudson, B.; Mayne, L. *Methods Enzymol.* **1986**, *130*, 331. d. Hudson, B. *Spectroscopy* **1986**, *1*, 22.
(3) Harmon, P. A.; Asher, S. A. *J. Chem. Phys.* **1988**, *88*, 2925–38.
(4) Miller, F. A.; Kauffman, G. B. *J. Chem. Educ.* **1989**, *66*, 795–801.
(5) Strekas, T. C.; Spiro, T. G. *Biochim. Biophys. Acta* **1972**, *263*, 830.
(6) a. Spiro, T G.; Smulevich, G.; Su, C. *Biochemistry* **1990**, *29*, 4497. b. Asher, S. A. *Methods Enzymol.* **1981**, *76*, 372–413.
(7) Mathies, R. A.; Smith, S. O.; Palings, I. In *Biological Applications of RS*; Spiro, T. G., Ed.; John Wiley and Sons: New York, 1987; Vol. II.
(8) Garrell, R. L. *Anal. Chem.* **1989**, *61*, 401 A.
(9) Chase, B. *Anal. Chem.* **1987**, *59*, 881 A.
(10) Asher, S. A.; Johnson, C. R. *Science* **1984**, *225*, 311–13.
(11) Dudik, J. M.; Johnson, C. R.; Asher, S. A. *J. Chem. Phys.* **1985**, *82*, 1732–40.
(12) a. Asher, S. A.; Johnson, C. R.; Murtaugh, J. *Rev. Sci. Instrum.* **1983**, *54*, 1657–62. b. Ziegler, L. D.; Hudson, B. S. *J. Chem. Phys.* **1981**, *74*, 982.
(13) Jones, C. M.; DeVito, V. L.; Harmon, P. A.; Asher, S. A. *Appl. Spectrosc.* **1987**, *41*, 1268–75.
(14) a. Williams, K.P.J.; Klenerman, D. J. *Raman Spectrosc.* **1992**, *23*, 191. b. Gustafson, T. L. *Optics Comm.* **1988**, *67*, 53.
(15) Asher, S. A.; Bormett, R. W.; Chen, X. G.; Lemmon, D. H.; Cho, N.; Peterson, P.; Arrigoni, M.; Spinelli, L.; Cannon, J., submitted for publication in *Appl. Spectrosc.*
(16) Rodgers, K. R.; Su, C.; Subramaniam, S.; Spiro, T. G. *J. Am. Chem. Soc.* **1992**, *114*, 3697–3709.
(17) a. Zhang, Y. P.; Ziegler, L. D. *J. Phys. Chem.* **1989**, *93*, 6665. b. Ziegler, L. D. *J. Chem. Phys.* **1987**, *86*, 1703. c. Phillips, D. L.; Myers, A. B. *J. Chem. Phys.* **1991**, *95*, 226. d. Li, B.; Myers, A. B. *J. Chem. Phys.* **1991**, *94*, 2458. e. Phillips, D. L.; Myers, A. B.; Valentini, J. J. *J. Phys. Chem.* **1992**, *96*, 2039–44.
(18) Ci, X.; Myers, A. B. *Chem. Phys. Lett.* **1989**, *158*, 263–69.
(19) DeVito, V. L.; Asher, S. A. *J. Am. Chem. Soc.* **1989**, *111*, 9143–52.
(20) Sension, R. J.; Hudson, B. S. *J. Chem. Phys.* **1989**, *90*, 1377.
(21) Ziegler, L. D.; Hudson, B. S. *J. Chem. Phys.* **1983**, *79*, 1134.
(22) DeVito, V. L.; Cai, M-Z.; Asher, S. A.; Kehres, L. A.; Smith, K. M. *J. Phys. Chem.* **1992**, *96*, 6917–22.